Molecular Design and Polymer Structure Control Based on Polymer Crystal Engineering. Topochemical Polymerization of 1,3-Diene Mono- and Dicarboxylic Acid Derivatives Bearing a Naphthylmethylammonium Group as the Countercation

Akikazu Matsumoto,* Sadamu Nagahama, and Toru Odani

Contribution from the Department of Applied Chemistry, Faculty of Engineering, Osaka City University, Sugimoto, Sumiyoshi-ku, Osaka 558-8585, Japan

Received March 28, 2000

Abstract: The topochemical polymerization of the alkylammonium salts of *(Z,Z)*-, *(E,Z)*-, and *(E,E)*-1,3-diene mono- or dicarboxylic acids, i.e., of the muconic and sorbic acid derivatives, is described from the viewpoint of polymer crystal engineering. Not only the *(Z,Z)*- but also the *(E,E)*-derivatives polymerize to give a high molecular weight polymer in the crystalline state under UV irradiation when a naphthylmethylammonium moiety is introduced to these monomers as the countercation. NMR spectroscopy confirms the formation of the stereoregular *meso*- or *erythro*-diisotactic-*trans*-2,5-polymer during the polymerization, irrespective of the configuration of the monomers and the structure of the substituents. The single-crystal structure analysis of the naphthylmethylammonium salt of sorbic acid reveals the stacking of the diene moieties in the columns formed in the crystals, favorable for the topochemical polymerization. The photopolymerization reactivity and the stereochemistry of the resulting polymers are determined by the molecular packing in the crystals during the topochemical polymerization of the diene monomers.

Introduction

In recent years, many reports have been published on the polymer structure control by radical polymerization, which is the most convenient and important process for the production of vinyl polymers because of the advantageous features of polymerization. In contrast to the recent progress in the control of the molecular weight and molecular weight distribution and of the structures of the α- and ω-chain ends and branching using the living radical polymerization technique,[1] the control of tacticity is still difficult due to the free radical propagating species. Several organized media such as liquid crystals, inclusion compounds, and molecular crystals have been used for the synthesis of polymers with a well-defined chain structure,[2] as well as specially designed monomers affording a stereoregular polymer through radical polymerization in isotropic medium.[3] Topochemical polymerization in the crystalline state is the most promising method for controlling the stereochemistry of polymer chains, and to give polymer crystals with a structure that is strictly determined by the crystal structure of the monomers.[4] In 1994, we discovered a new type of topochemical polymerization of a 1,3-diene monomer,[5] although very few examples have been found to undergo the topochemical polymerization. We have demonstrated that the diethyl ester[6−10] and several alkylammoniums[11−14] of *(Z,Z)*-muconic acid provide ultrahigh molecular weight and stereoregular polymers under UV irradiation in the crystalline state (Scheme 1). This polymerization has the following several features: The polymerization proceeds via a radical chain polymerization mechanism, induced by the irradiation of UV light or higher energy

* Address correspondence to this author. Phone: +81-6-6605-2981. Fax: +81-6-6605-2981. E-mail: matsumoto@a-chem.eng.osaka-cu.ac.jp.

(1) (a) Otsu, T.; Matsumoto, A. *Adv. Polym. Sci.* **1998**, *136*, 75−137. (b) Matyjaszewski, K., Ed. *Controlled Radical Polymerization*; ACS Symp. Ser. No. 685; American Chemical Society: Washington, DC, 1998. (c) Moad, G.; Solomon, D. H. *The Chemistry of Free Radical Polymerization*; Pergamon: Oxford, 1995.

(2) (a) Paleos, C. M., Ed. *Polymerization in Organized Media*; Gordon and Breach: Philadelphia, 1992. (b) Miyata, M. *Comprehensive Supramolecular Chemistry*; Reinhoudt, N. D., Ed.; Pergamon: Oxford, 1996; Vol. 10, pp 557−582. (c) Stupp, S. I.; Osenar, P. *Synthesis of Polymers*; Schlüter, A.-Dieter, Ed.; Wiley-VCH: Weinheim, 1999; pp 513−547.

(3) (a) Okamoto, Y.; Nakano, T. *Chem. Rev.* **1994**, *94*, 349−372. (b) Porter, N. A.; Allen, T. R.; Breyer, R. A. *J. Am. Chem. Soc.* **1992**, *114*, 7676−7683.

(4) (a) Schmidt, G. M. J. *Pure Appl. Chem.* **1971**, *27*, 647−678. (b) Wegner, G. *Pure Appl. Chem.* **1977**, *49*, 443−454. (c) Enkelmann, V. *Adv. Polym. Sci.* **1984**, *63*, 91−136. (d) Hasegawa, M. *Adv. Phys. Org. Chem.* **1995**, *30*, 117−171. (e) Venkatesan, K.; Ramamurthy, V. *Photochemistry in Organized and Constrained Media*; Ramamurthy, V., Ed.; VCH: New York, 1991; Chapter 4, pp 133−184.

(5) (a) Matsumoto, A.; Matsumura, T.; Aoki, S. *J. Chem. Soc., Chem. Commun.* **1994**, 1389−1390. (b) Matsumoto, A.; Matsumura, T.; Aoki, S. *Macromolecules* **1996**, *29*, 423−432. (c) Matsumoto, A.; Odani, T. *Controlled/Living Radical Polymerization*; ACS Symp. Ser. No. 768; Matyjaszewski, K., Ed.; American Chemical Society: Washington, DC, 2000; Chapter 7; pp 93−106.

(6) Matsumoto, A.; Yokoi, K.; Aoki, S.; Tashiro, K.; Kamae, T.; Kobayashi, M. *Macromolecules* **1998**, *31*, 2129−2136.

(7) Tashiro, K.; Kamae, T.; Kobayashi, M.; Matsumoto, A.; Yokoi, K.; Aoki, S. *Macromolecules* **1999**, *32*, 2449−2454.

(8) Tashiro, K.; Zadorin, A. N.; Saragai, S.; Kamae, T.; Matsumoto, A.; Yokoi, K.; Aoki, S. *Macromolecules* **1999**, *32*, 7946−7950.

(9) Matsumoto, A.; Katayama, K.; Odani, T.; Oka, K.; Tashiro, K.; Saragai, S.; Nakamoto, S. *Macromolecules*, in press.

(10) (a) Matsumoto, A.; Yokoi, K.; Aoki, S. *Polym. J.* **1998**, *30*, 361−363. (b) Matsumoto, A.; Yokoi, K. *J. Polym. Sci., Part A, Polym. Chem.* **1998**, *36*, 3147−3155.

(11) Matsumoto, A.; Odani, T.; Aoki, S. *Polym. J.* **1998**, *30*, 358−360.

(12) Matsumoto, A.; Yokoi, K.; Odani, T. *Proc. Jpn. Acad., Ser. B* **1998**, *74*, 110−115.

(13) Matsumoto, A.; Odani, T.; Chikada, M.; Sada, K.; Miyata, M. *J. Am. Chem. Soc.* **1999**, *121*, 11122−11129.

(14) Matsumoto, A.; Odani, T.; Sada, K.; Miyata, M.; Tashiro, K. *Nature* **2000**, *405*, 328−330. (b) Ward, M. D. *Nature* **2000**, *405*, 293−294.

10.1021/ja001093n CCC: $19.00
Published on Web 09/06/2000

Scheme 1

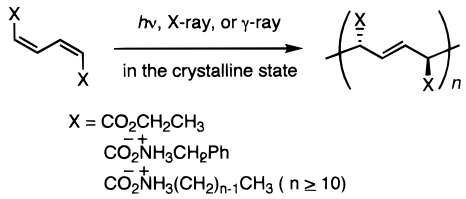

rays such as X-rays and γ-rays. A very high molecular weight polymer is produced during the polymerization and the molecular weight of the polymer depends on the size of the monomer crystals. The most important feature of the polymerization is the control of the polymer stereochemistry. A tritactic polymer with a regulated structure is formed, i.e., the tacticity of two asymmetric carbon centers and a double bond is completely controlled during the topochemical polymerization of the muconate as the 1,4-disubstituted butadiene derivative. Furthermore, we can isolate polymers in the form of polymer crystals after polymerization, as the polymer single crystals under appropriate conditions.

The process of topochemical polymerization has recently been confirmed by the determination of the single-crystal structure of both the monomer and polymer,[8,13] and by structural change during polymerization using IR and Raman spectroscopies as well as X-ray diffraction.[6,7] The molecular packing types in the crystals of a series of benzylammonium salts and its related derivatives were classified into columnar-type and sheet-type molecular arrangements, which are closely related to the pattern of hydrogen bond networks. They are correlated with their photoreaction behavior in the crystalline state. The polymerizable monomer molecules form a columnar assembly in the crystals and a polymer chain is produced along the column via a topochemical polymerization mechanism. In the topochemical reaction, the reaction pathway and its reactivity intrinsically depend on the monomer crystal structure as the starting materials. Therefore, to design any topochemically polymerizable ammonium monomer other than the benzylammonium derivatives, it is necessary that the cation parts strongly stack upon each other to support a columnar structure of the muconate dianions without disturbing the ideal crystal structure for the topochemical polymerization, i.e., a favorable distance between the reacting double bonds and a favorable tilt angle of the diene moiety to the column. If there is any guide for the structural design of the diene monomers appropriate for topochemical polymerization, it would be very useful for the control and design of the polymer structures obtained therefrom as the photoproducts. A naphthylmethylammonium moiety seemed to be suitable for this purpose. In fact, we have recently found that the 1-naphthylmethylammonium salts of the *(E,E)*-muconic and sorbic acids photopolymerized in the crystalline state and provided stereoregular polymers, as well as the *(Z,Z)*-muconic acid derivatives.[15,16]

Crystal engineering, which is the planning of syntheses in the crystalline state and the evaluation of the structure and properties of the crystalline products, has been developed in the boundary areas of many research fields of organic, inorganic, organometallic, and material chemistry as well as biochemistry.[17−19] We can see marvelous progress in crystal engineering based on the supramolecular synthon in recent years. However, it has less often been applied to polymer synthesis, despite the pioneering works concerning the topochemical polymerization of diolefins[4,20] and diacetylenes[4,21] discovered in the 1960s. From the viewpoint of controlled polymer synthesis, crystal engineering is very useful for the control of tacticity and molecular weight as the primary structure of polymers and of polymer crystalline structures. The prediction of the reactivity and the structure of polymers as the products is very important for the design of new organic solid materials. Here, we report the details of the topochemical polymerization of the 1-naphthylmethylammonium salts of several 1,3-diene mono- and dicarboxylic acid derivatives, i.e., three kinds of muconate isomers (**1**−**3**), monomethyl *(Z,Z)*- and *(E,E)*-muconates (**4** and **5**), and *(E,E)*-sorbate (**6**), as shown in Figure 1. The photopolymerization reactivity of the diene monomers and the stereochemistry of the obtained polymers are discussed based on the monomer configuration and molecular packing in the crystals.

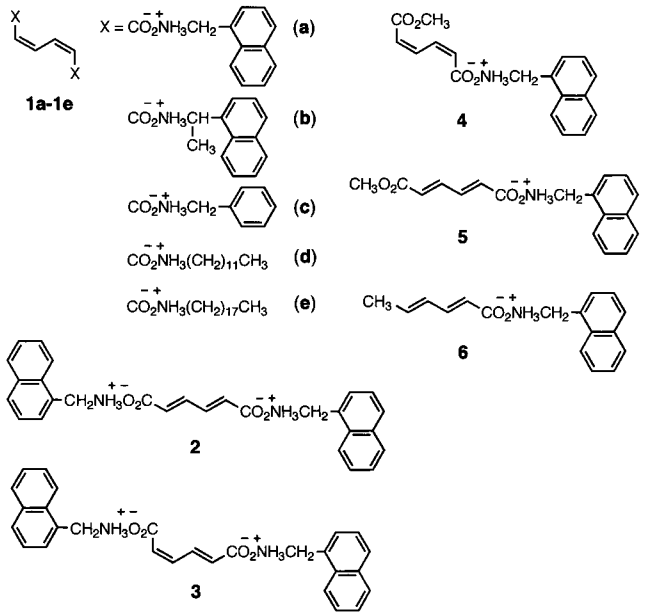

Figure 1. Chemical structure of the 1,3-diene monomers used in this study.

Results

Photoreaction Behavior. The photoreaction of the ammonium salts was carried out in the crystalline state under

(15) Preliminary results for the polymerization of **1a** and **2**: Odani, T.; Matsumoto, A. *Macromol. Rapid Commun.* **2000**, *21*, 40−44.

(16) Preliminary results for the polymerization of **6**: Matsumoto, A.; Odani, T. *Polym. J.* **1999**, *31*, 717−719.

(17) (a) Desiraju, G. R., Ed. *The Crystal as a Supramolecular Entity: Perspective in Supramolecular Chemistry*; Wiley: Chichester, 1996; Vol. 2. (b) Seddon, K. R.; Zaworotko, M. J., Eds. *Crystal Engineering: The Design and Application of Functional Solids*; NATO ASI Series C, Vol. 539; Kluwer Academic: Dordrecht, The Netherlands, 1999. (c) Braga, D.; Grepioni, F.; Orpen, A. G., Eds. *Crystal Engineering: From Molecules and Crystals to Materials*; NATO ASI Ser. C, Vol. 538; Kluwer Academic: Dordrecht, The Netherlands, 1999.

(18) (a) Desiraju, G. R. *Angew. Chem., Int. Ed. Engl.* **1995**, *34*, 2311−2327. (b) Hosseini, M. W.; DeCian, A. *Chem. Commun.* **1998**, 727−733. (c) Desiraju, G. R. *Chem. Commun.* **1997**, 1475−1482. (d) Aakeröy, C. B. *Acta Crystallogr.* **1997**, *B53*, 569−586. (e) Nangia, A.; Desiraju, G. R. *Top. Cur. Chem.* **1998**, *198*, 57−95. (f) Braga, D.; Grepioni, F.; Desiraju, G. R. *Chem. Rev.* **1998**, *98*, 1375−1405. (g) Rogers, R. D.; Zaworotko, M. J. *Trans. Am. Crystallogr. Assoc.* **1998**, *33*, 1−5.

(19) (a) Lehn, J.-M. *Supramolecular Chemistry*; VCH: Weinheim, 1995. (b) MacNicol, D. D.; Toda, F.; Bishop, R., Eds. *Comprehensive Supramolecular Chemistry*; Pergamon: Oxford, 1996; Vol. 6.

(20) (a) Hasegawa, M.; Suzuki, Y. *J. Polym. Sci. B* **1967**, *5*, 813−815. (b) Nakanishi, H.; Hasegawa, M.; Sasada, Y. *J. Polym. Sci., Part A-2* **1972**, *10*, 1537−1553. (c) Nakanishi, H.; Hasegawa, M.; Sasada, Y. *J. Polym. Sci., Polym. Lett. Ed.* **1979**, *17*, 459−462.

(21) (a) Wegner, G. *Z. Naturforsch.* **1969**, *24B*, 824−832. (b) Wegner, G. *J. Polym. Sci., Polym. Lett. Ed.* **1971**, *9*, 133−144. (c) Wegner, G. *Makromol. Chem.* **1971**, *145*, 85−94. (d) Baughman, R. H.; Yee, K. C. *J. Polym. Sci., Macromol. Rev.* **1978**, *13*, 219−239. (e) Bloor, D. *Developments in Crystalline Polymers II*; Bassett, D. C., Ed.; Applied Science Publishers: London, 1982; pp 151−193.

Table 1. Photopolymerization of Alkylammonium Muconates and Sorbates in the Crystalline State with a High-Pressure Mercury Lamp at Room Temperature

run	monomer	time (h)	polymer yield (%)	$[\eta]^a \times 10^{-2}$ (cm³/g)	isomer composition of monomer recovered (Z,Z)-	(E,Z)-	(E,E)-
1	**1a**	8	90	1.47	100	0	0
2	**1b**	8	0		100	0	0
3	**1c**[b]	8	21	12.7[c]	100	0	0
4	**1d**[d]	8	80	4.61[c]	100	0	0
5	**1e**[d]	8	95		100	0	0
6	**2**	8	71	0.96	0	0	100
7	**3**	8	trace		0	91	9
8	**3**	40	8		0	86	14
9	**4**[e]	35	trace		18	18	64
10	**4**[e]	100	15		0	9	91
11	**5**	8	59	2.05	0	0	100
12	**6**	8	98	14.1	0	0	100

[a] In methanol at 30 °C. Measured as the triethylammonium polymer after solid-state polymer transformation (see Scheme 3). [b] Reference 13. [c] In 0.5 M aqueous NaCl at 30 °C. Measured as the *n*-propylammonium polymers after solid-state polymer transformation. [d] Reference 14. [e] The monomer **4** was contaminated by the *(E,Z)*-isomer: *(Z,Z)-/(E,Z)-/(E,E)-* = 86/14/0 before photoirradiation.

photoirradiation with a high-pressure mercury lamp for 8 h at room temperature under atmospheric conditions. The naphthylmethylammonium salt of *(Z,Z)*-muconic acid **1a** provided the polymer in high yield (run 1 in Table 1), similar to the results for the benzyl- and *n*-alkylammonium salts (runs 3−5). The corresponding *(E,E)*-isomer **2** also yielded a polymer in high yield (run 6), in contrast to the fact that the other *(E,E)*-derivatives were inert during the photoirradiation. When the unreacted monomer was checked by NMR spectroscopy after the polymerization of **1a** and **2**, only the original isomer was detected in each case. This indicates that each monomer polymerized without any isomerization. Differing from the high polymerization reactivity of the naphthylmethylammonium derivatives, **1b** did not give any polymer despite the similar structure of the *N*-substituents (run 2). A drastic change in photoreaction behavior induced by a small change in the structure of the substituents is observed for other systems, e.g., the topochemical polymerization ability disappeared when an α-methyl group was introduced to **1c**.[13] The photoreaction of the *(E,Z)*-monomers was also investigated, but they produced the corresponding *(E,E)*-isomers in very low yield. When the photoirradiation of **3** was carried out for a long time, a polymer was produced in low yield (run 8). There are two possible pathways for the formation of the polymer. One possibility is the direct polymerization of **3**. Another is the polymerization via the isomerization to the corresponding *(E,E)*-isomer **2**. We considered that **3** first isomerized to **2**, followed by the polymerization, judging from the change in the composition of the recovered isomers and in the polymer yield depending on the photoirradiation time.

The irradiation of **4** as the *(Z,Z)*-derivative also afforded two kinds of photoproducts, an isomerized product and a polymer (runs 9 and 10),[22] being different from the photoreaction of **1a** giving a polymer without isomerization. When the polymerization reactivity of **5** was checked in the crystalline state, the polymer was produced in high yield under similar conditions, and no isomerization to **4** occurred (run 11). The time dependence of the composition of the photoproducts during the reaction of **4** suggested that **4** does not polymerize, but isomerizes to **5** in the crystalline state during photoirradiation. We also examined the photoreaction behavior of the ammonium salt crystals of *(E,E)*-sorbic acid, because the crystalline-state polymerization of the *(E,E)*-muconic acid derivatives inspired us to investigate the other types of 1,3-diene monomers. Consequently, we have found that **6** polymerized in the crystalline state (run 12), while other derivatives such as the *n*-butyl-, isopropyl-, *tert*-butyl-, and benzylammonium salts had no reactions. Thus, it has been demonstrated that the introduction of the naphthylmethylammonium moiety is very effective for inducing the topochemical polymerization of not only the muconic acid but also the sorbic acid derivatives, and of both isomers of the *(Z,Z)*- and *(E,E)*-derivatives.

Scheme 2

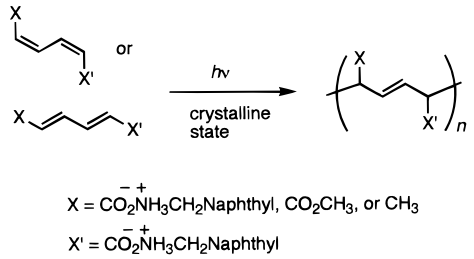

Chemical Structure of Polymer Chains. The polymers obtained in this study have the *trans*-2,5-structure as the repeating unit, as shown in Scheme 2, irrespective of the monomer configuration and the substituents. In the IR spectra of the polymers, the shift in the peak due to the carbonyl stretching and the appearance of the out-of-plane deformation vibration due to the *trans*-CH═CH moiety were confirmed. The polymers bearing the naphthylmethylammonium group as the countercation in the side chain were insoluble in all solvents including polar organic solvents, alkaline solutions, and acids, similar to previously reported poly(**1c**).[13] Therefore, the polymers were converted to the triethylammonium derivatives through a solid-state polymer transformation to determine the structure of the polymers in solution.

First, the original ammonium polymers were converted to poly(muconic acid), its monomethyl ester, or poly(sorbic acid) through the solid-state hydrolysis, which proceeded heterogeneously because both the ammonium and acid polymers were insoluble in methanol. The quantitative transformation was confirmed by IR spectroscopy and elemental analysis. Subsequently, the polyacids were again converted to the ammonium salt polymers (Scheme 3). All the triethylammonium polymers (poly(**7**)−poly(**9**)) were soluble in methanol and water.

The triethylammonium polymers were used for the ^{13}C NMR measurement in methanol-d_4 to characterize the stereochemical structure of the polymers. Figure 2a−c shows the NMR spectra of poly(**7**), poly(**8**), and poly(**9**), which were derived from poly(**2**), poly(**5**), and poly(**6**), respectively, through the polymer transformation. The narrow and single peaks for each carbon observed in the spectra indicate the formation of a stereoregular polymer during the crystalline-state polymerization. The spectrum of the polymer derived from **2** as the starting monomer was identical with that from **1a** or **1c**. The spectra of the stereoregular polymers produced by topochemical polymerization are much different from the broad spectrum of the atactic polymers that were prepared by solution polymerization of the acid and the subsequent salt formation (Scheme 4),[13] and by the free-radical or group-tranfer polymerization of the ester derivatives.[5,23] From the chemical shifts and the previous results for the other related polymers,[24] it has been revealed that the polymers obtained during the topochemical polymerization have

(22) The *(E,Z)*-isomer seemed to photoisomerize to **5** at a much lower rate, compared with the isomerization of **4** to **5**, although the **4** crystals were contaminated by a small amount of the *(E,Z)*-isomer.

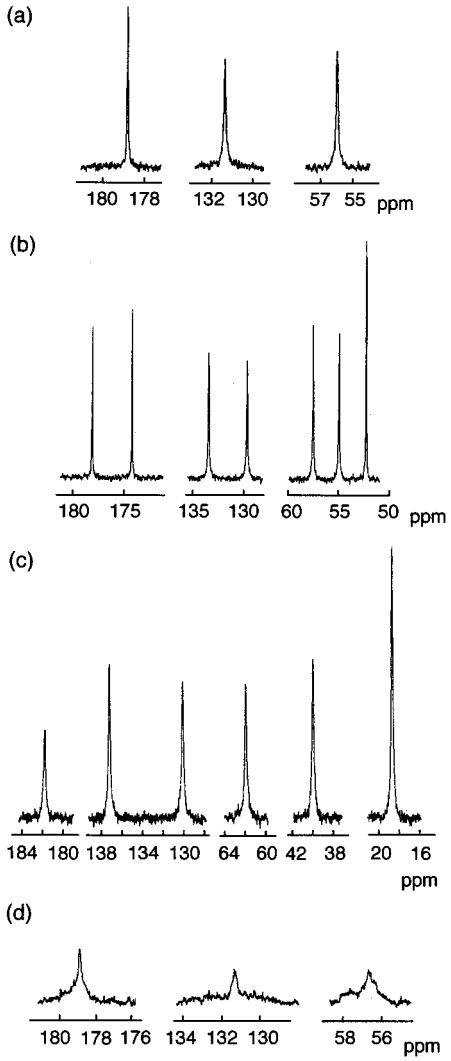

Figure 2. ^{13}C NMR spectra of triethylammonium polymers: (a) poly(**7**) derived from poly(**2**), (b) poly(**8**) derived from poly(**5**), (c) poly(**9**) derived from poly(**6**), and (d) atactic poly(**7**) derived from the polymer produced during the polymerization of **3** via the isomerization (run 8 in Table 1). Measurement solvent, methanol-d_4.

Scheme 3

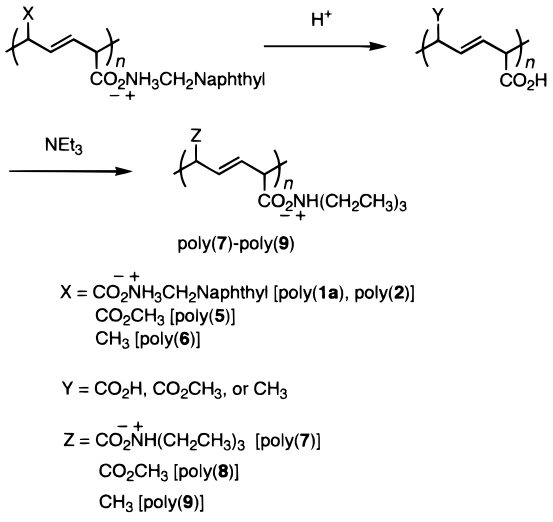

a similar structure, that is, a *meso*- or *erythro*-diisotactic-*trans*-2,5-structure (vide infra), irrespective of the configuration of the monomers.

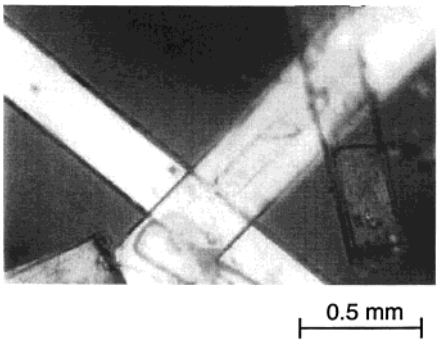

Figure 3. Microphotograph of the monomer crystals of **6**.

Scheme 4

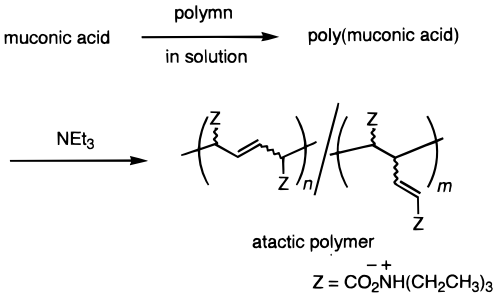

Polymerization Reactivity in the Crystalline State. In a similar way, the molecular weight of the resulting polymers was estimated after converting the polymer to the soluble polymers. The viscosity data in Table 1 suggest that high molecular weight polymers were formed during the crystalline-state photopolymerization of the naphthylmethylammonium derivatives. The value of the intrinsic viscosity, i.e., the molecular weight of the polymer, seemed to be dependent on the crystal size rather than the reactivity of the monomer used. Namely, **6** was isolated as large-size needles (Figure 3), resulting in an identical shape of the polymer crystals after the topochemical polymerization. The polymer produced from the crystals of **6** was of the highest molecular weight polymer ($[\eta] = 1.4 \times 10^3$ cm^3/g in methanol). The polymerization of the needle crystals of **1c** also resulted in the formation of a high molecular weight polymer ($[\eta] = 1.3 \times 10^3$ cm^3/g), whereas the other naphthylmethylammonium derivatives, **1a**, **2**, and **5** were obtained as fine powder crystals, having lower $[\eta]$ values of the polymers obtained therefrom ($[\eta] = (1-2) \times 10^2$ cm^3/g).

It has been demonstrated that the molecular weight of the polymer can be controlled by the crystal size during the topochemical polymerization.[10,25] It was also pointed out that the monomer crystal size influences not only the molecular weight but also the yield of the polymer produced.[9,10] Therefore, we compared the polymerization reactivity as thin crystal samples by IR spectroscopy using the KBr disk method. The thin monomer crystals dispersed in KBr were irradiated in high efficiency independent of the kind of monomers. Figure 4 shows

(23) (a) Matsumoto, A.; Horie, A.; Otsu, T. *Makromol. Chem., Rapid Commun.* **1991**, *12*, 681−685. (b) Hertler, W. R.; RajanBabu, T. V.; Ovenall, D. W.; Reddy, G. S.; Sogah, D. Y. *J. Am. Chem. Soc.* **1988**, *110*, 5841−5853.

(24) (a) Wang, X.; Komoto, T.; Ando, I.; Otsu, T. *Makromol. Chem.* **1988**, *189*, 1845−1854. (b) Yoshioka, M.; Matsumoto, A.; Otsu, T.; Ando, I. *Polymer* **1991**, *32*, 2741−2746. (c) Rätzsch, M.; Zschoche, S.; Steinert, V.; Schlothauer, K.; Kamatani, H. *Makromol. Chem.* **1986**, *187*, 1669−1679.

(25) (a) Iida, R.; Kasai, H.; Okada, S.; Oikawa, H.; Matsuda, H.; Kakuta, A.; Nakanishi, H. *Mol. Cryst. Liq. Cryst.* **1995**, *267*, 95−100. (b) Katagi, H.; Kasai, H.; Okada, S.; Oikawa, H.; Komatsu, K.; Matsuda, H.; Liu, Z.; Nakanishi, H. *Jpn. J. Appl. Phys., Part 2, Lett.* **1996**, *35*, 1364−1366.

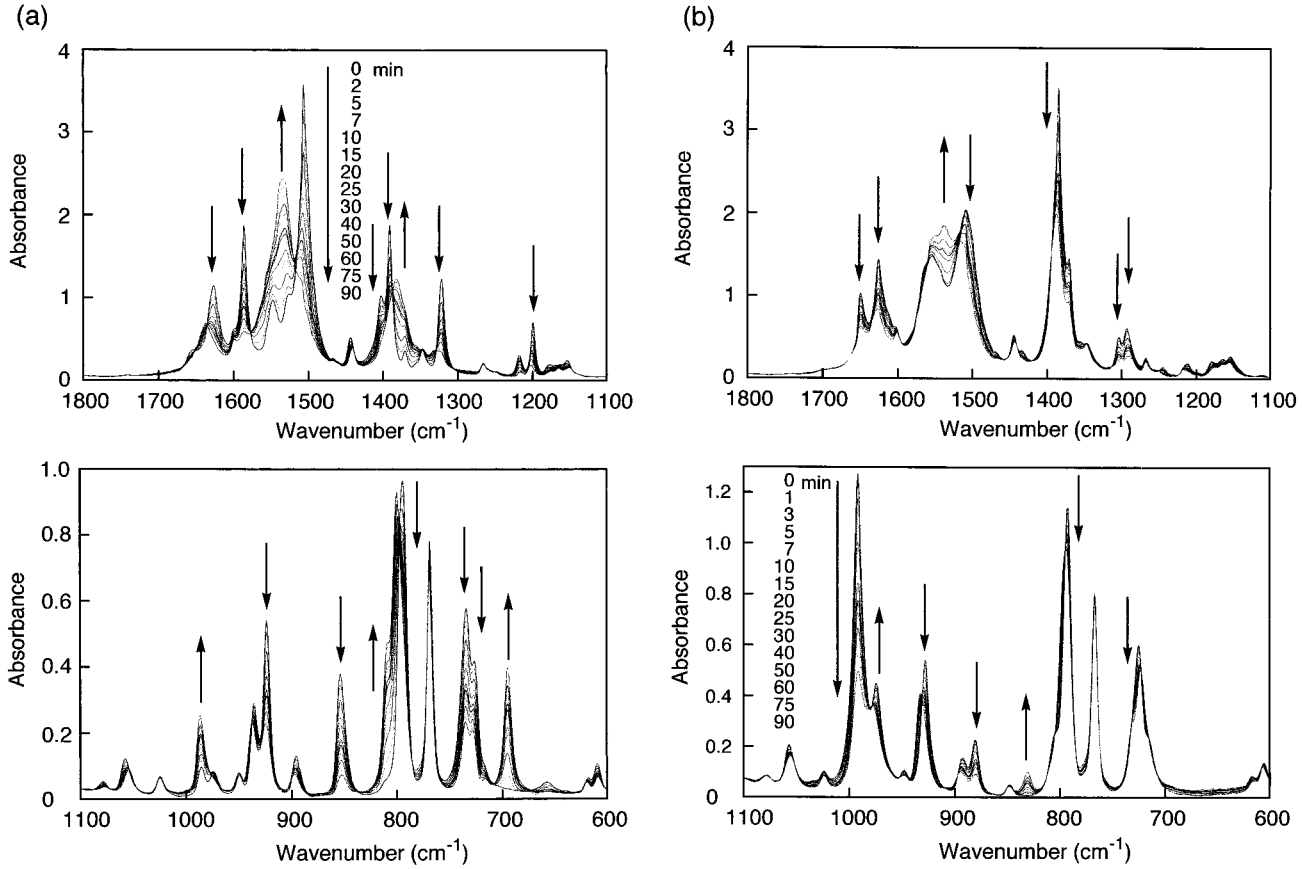

Figure 4. Change in the IR spectra during photopolymerization in the crystalline state: (a) **1a** and (b) **6**. The irradiation of the KBr disk samples was carried out with a high-pressure mercury lamp at a distance of 10 cm at room temperature. The photoirradiation time was 0−90 min.

typical examples of the spectrum change during the photoirradiation in the crystalline state under identical photoirradiation conditions: intensity of light, distance from a light source, and temperature. The peaks due to the monomers decreased and those of the polymers increased along with the irradiation time. In these cases, the spectrum change can be considered a simple two-component system, i.e., the spectrum observed during the reaction consists of the components due to both the monomer and polymer.[7] We determined the rate of the polymerization from the intensity change in some characteristic bands using the relative intensities in the peaks due to the monomer and polymer. The semilogarithmic plots of the relative concentration of the monomer (C_t/C_0) during the polymerization of some derivatives are shown in Figure 5. The slope of the lines gives the apparent first-order kinetic reaction constant (k) with regard to the monomer fraction during the crystalline-state polymerization. The details of the analytical method have already been shown in a previous paper.[7] The kinetic values determined for several monomers are listed in Table 2.

Monomer and Polymer Crystal Structures. When the powder X-ray diffraction profiles were recorded for the monomer crystals as well as the resulting polymer crystals, it was confirmed that the sharpness and intensity of the diffraction was retained even after the polymerization, and the diffraction pattern of the polymer closely resembled that of the respective monomer. In Table 3, the characteristic peaks observed in a low-angle region in the diffraction and the calculated interplanar distance are summarized. The interplanar distance is the repeating period of the lamella structure consisting of the carboxylate layers and the countercation layers.[13,14] Next, we tried to determine the crystal structures of the naphthylmethylammonium derivatives, but failed due to the difficulty in the preparation of high-quality single crystals. Exceptionally, however, the crystal of **6** was easily isolated as large and single crystals sufficient for the X-ray crystal structure analysis, as shown in Figure 3. The crystal structure parameters determined for the crystal of **6** are summarized in Table 4, and compared with the results for the previously reported **1c**.[13]

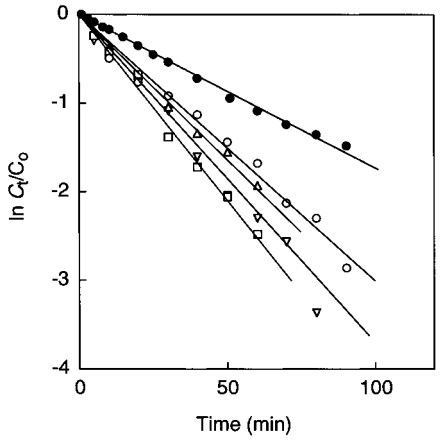

Figure 5. First-order kinetic plot during photopolymerization in the crystalline state: (a) **1a** (○), (b) **1c** (●), (c) **2** (□), (d) **5** (▽), and (e) **6** (△).

Discussion

Crystal Structure and Reactivity. The photoreaction pathways of monomers **1**−**5** in the crystalline state are summarized in Schemes 5 and 6. Both isomers **1a** and **2** polymerize in the crystalline state to give a polymer with an identical stereochemical structure. Compounds **3** and **4** have no polymerizability,

Table 2. First-Order Kinetic Reaction Constants for the Photopolymerization of Several Monomers in the Crystalline State[a]

monomer	$k \times 10^4$ (s^{-1})
1a	5.1 ± 0.5
1c	2.8 ± 0.2
2	7.0 ± 0.7
5	6.6 ± 0.5
6	5.6 ± 0.5
diethyl *(Z,Z)*-muconate	$33.9^b \pm 5.6$

[a] Determined by IR specroscopy with KBr disk. The photoirradiation was carried out with a high-pressure mercury lamp at a distance of 10 cm at room temperature. [b] Irradiated at a distance of 20 cm.

Table 3. Characteristic Peak Observed at a Low-Angle Region in a Powder X-ray Diffraction Profile for Monomer and Polymer Crystals of Muconic and Sorbic Acid Derivatives[a]

	monomer crystals		polymer crystals	
compd	2θ (deg)	d (Å)	2θ (deg)	d (Å)
1a	4.00	22.0	4.11	21.5
1c	5.12	17.3	5.20	17.0
	(5.10)[b]	(17.3)[b]		
1d[c]	2.63	33.6	2.79	31.7
1e[c]	1.93	45.8	2.02	43.7
2	3.97	22.3	4.05	21.8
5	5.87	15.1	2.94,[d] 5.89	30.1, 15.0
6	3.19,[d] 6.47	27.7, 13.7	3.21,[d] 6.47	27.5, 13.7
	(3.28, 6.56)[b]	(26.9, 13.5)[b]		

[a] With the Cu Kα line ($\lambda = 1.5418$ Å). [b] Calculated from the results of single-crystal structure analysis. [c] Determined by small-angle X-ray diffraction (ref 14). [d] Weak diffraction.

Table 4. Crystallographic Data for the Crystals of **6** and **1c**

compd	**6**	**1c**[a]
formula	$C_{17}H_{19}NO_2$	$C_{10}H_{12}NO_2$
formula weight	269.34	178.21
crystal system	monoclinic	monoclinic
space group	*C*2/*c*	$P2_1/a$
a, Å	54.642(3)	10.98(1)
b, Å	4.9909(1)	4.862(2)
c, Å	11.0533(1)	17.72(1)
β, deg	99.442(2)	97.93(9)
V, Å^3	2973.5(2)	936(1)
Z	8	4
D_c	1.203	1.264
no. of unique reflcns	3487	1430
no. observed reflcns	795	1090
R, R_w	0.066, 0.095	0.188, 0.313
GOF	1.04	1.23
$2\theta_{max}$, deg	55.0	51.2
R/*P*	4.39	9.24
P-facter	0.0500	0.200
temp, °C	23	−63

[a] Reference 13.

but provide the corresponding *(E,E)*-isomers **2** and **5**, respectively. The photoisomerization of the *(Z,Z)*-1,3-diene compounds to the corresponding *(E,E)*-derivatives in the crystalline state has already been reported for several other *(Z,Z)*-muconic acid derivatives including the esters, the amides, and the ammonium salts.[11−13] The isomerization proceeds one-way with an excellent stereospecificity from the *(Z,Z)*- to *(E,E)*-form in the crystalline state during photoirradiation. In contrast, the photoreaction in solution resulted in a mixture of more complicated photoproducts, indicating that a high selectivity during the isomerization is due to the crystal-lattice controlled reaction.

The kinetic results shown in Table 2 indicate that the derivatives bearing a naphthylmethylammonium group examined in this study have a similar polymerization reactivity in the crystalline state ($k = (5.1-7.0) \times 10^{-4}$ s^{-1}). The rate constants

Scheme 5

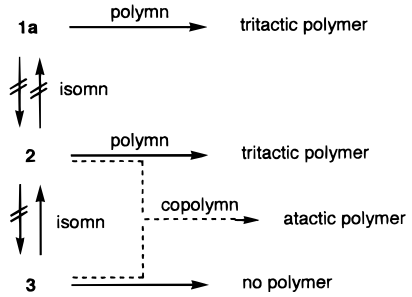

Scheme 6

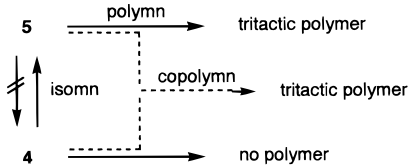

for the naphthylmethylammonium monomers are higher than the value for the benzylammonium salt (2.8×10^{-4} s^{-1}). The high polymerization reactivity of the naphthylmethylammonium derivatives supports the belief that the polymerization readily proceeds in the crystalline state when the cationic moieties of the ammonium muconates interact with each other to form robust columns in the crystals. The order of **2** ≥ **5** ≥ **6** ≥ **1a** > **1c** for the *k* value disagrees with the order of the polymer yield in Table 1. This is because the results in Table 1 imply the significant effect of the crystal size on the polymerization reactivity. The polymerization of the ammonium derivatives proceeded at a much lower rate, compared with the fast polymerization of the ethyl ester. It may be due to the molecular motion restricted by the two-dimensional (2D) hydrogen bond network in the crystals of the ammonium derivatives.[13] The polymerization rate depends on the crystal structure, more strictly, on the packing mode in a column formed in the monomer crystals, such as stacking distance, tilt angles, and intermolecular carbon-to-carbon distance.

Figure 6 shows the schematic molecular packing models for the polymerizable monomer crystals, **1c**, **1a**, and **2**, based on the *d*-values determined in this work and the previously reported crystal structure of **1c**. The *d*-value for **1a** (22.0 Å) being larger than that of **1c** (17.3 Å) is quite consistent with the structure based on the size of the ammonium groups. The *(E,E)*-muconate dianion has a slightly greater molecular axis length compared with the *(Z,Z)*-muconate dianion. The *d*-value for **2** (22.3 Å) may imply the difference in the molecular size of the muconates. An asymmetric type of ammonium carboxylate monomer such as **5** or **6** possibly favors a more complicated packing pattern. When the interaction between the naphthyl groups is important, the molecular packing is similar to those for the diammonium derivatives shown in Figure 6, whereas an interaction between the alkyl and aromatic groups would result in another crystal form. From the comparison of the *d*-values of the monomer and polymer crystals for each compound (Table 3), it has been clarified that the thickness of the lamella does not change, supporting the belief of a topochemical reaction process. A slight decrease in the *d*-values for the polymer crystals is due to the rotation of the diene moieties during the polymerization. This has been confirmed by the crystal structure determination of both the monomer and polymer of the ethyl ester of *(Z,Z)*-muconic acid.[8] For the crystals of a series of *n*-alkylammonium *(Z,Z)*-muconates including **1d** and **1e**, the lamella structure of the monomers and polymers was characterized in detail in a

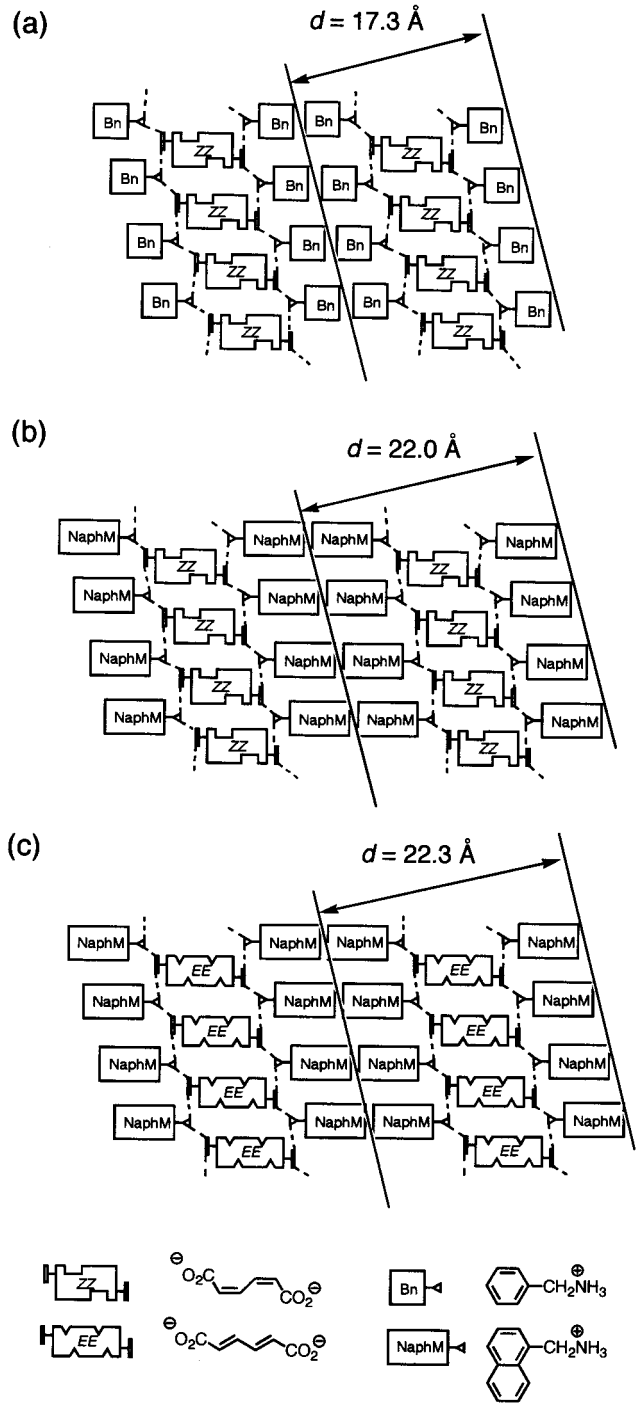

Figure 6. Schematic models for the monomer crystals of the diammonium muconates: (a) **1c**, (b) **1a**, and (c) **2**. The dotted lines show the two-dimensional hydrogen bond networks formed between the ammonium cations and the carboxylate anions. The diene moieties stack to make columns in a direction perpendicular to the paper sheet, and the polymers are formed along the column during the photopolymerization.

previous work.[14] It has been proved that the naphthylmethylammonium moiety is also a good countercation for constructing a lamella-type crystal structure, consisting of the butadiene mono- or dicarboxylate anion layers and the countercation layers, favorable for the topochemical polymerization.

The crystal structure of **6** viewed down the crystallographic *b*- and *c*-axes is shown in Figure 7. The naphthyl and sorbate moieties stack in the direction of the *b*-axis to make each column. The lamella structure consisting of the sorbate anion

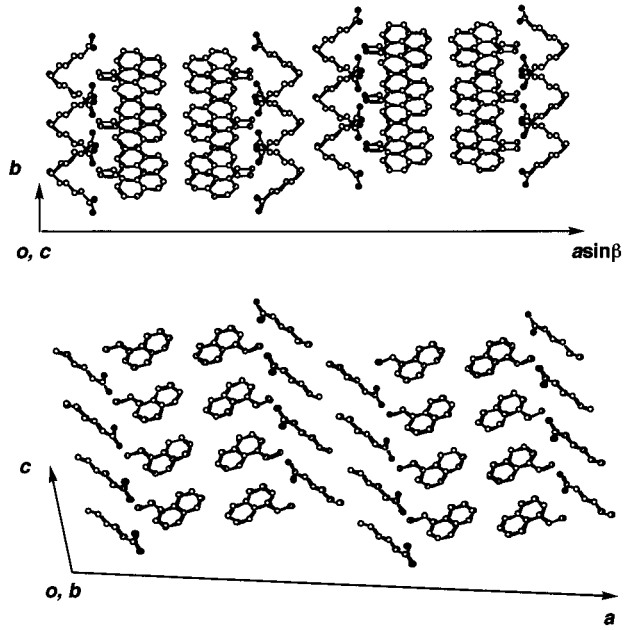

Figure 7. Crystal structure of **6** viewed from the crystallographic *b*- and *c*-axes. Hydrogen atoms are omitted for clarity.

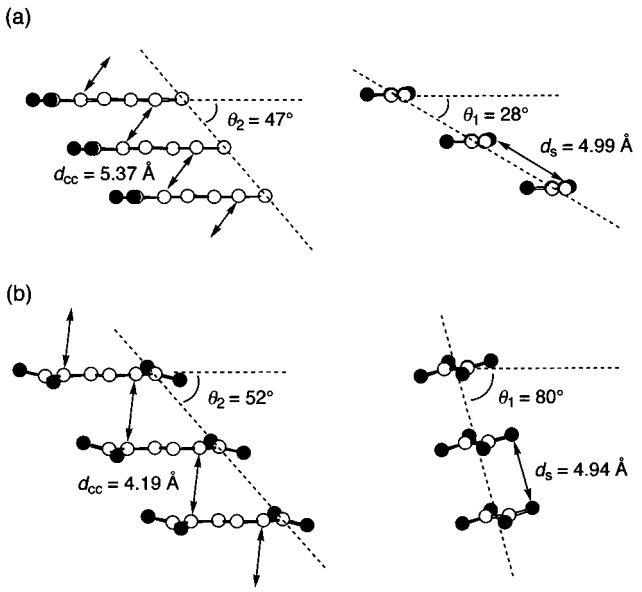

Figure 8. Molecular stacking in the column of the crystals: (a) **6** and (b) **1c**. Side and tail views of the molecular plane of the sorbate or muconate are shown.

layers and the naphthylmethylammonium layers is supported by the 2D hydrogen bond network, which runs along the *bc* face in the crystals. This is very similar to the molecular stacking observed in the crystal of **1c**.[13] Namely, the sorbate anions are arranged along the *b*-axis to make columns, which are linked by 2D hydrogen bond networks at an interface of the naphthylmethylammonium layers. The hydrogen bond network consists of the primary ammonium cations and the carboxylate anions, which act as triple hydrogen bond donors and triple hydrogen bond acceptors, respectively, as was observed for the crystals of the muconates.

Figure 8 shows the molecular stacking of the sorbate anions in the crystal of **6** and of the muconate anions in the crystal of **1c**. Several parameters that represent the characteristics of the molecular stacking in the crystal structure are shown in Table 5. The d_{cc} and d_s values are defined as the intermolecular carbon-to-carbon distance between the double bonds that react during

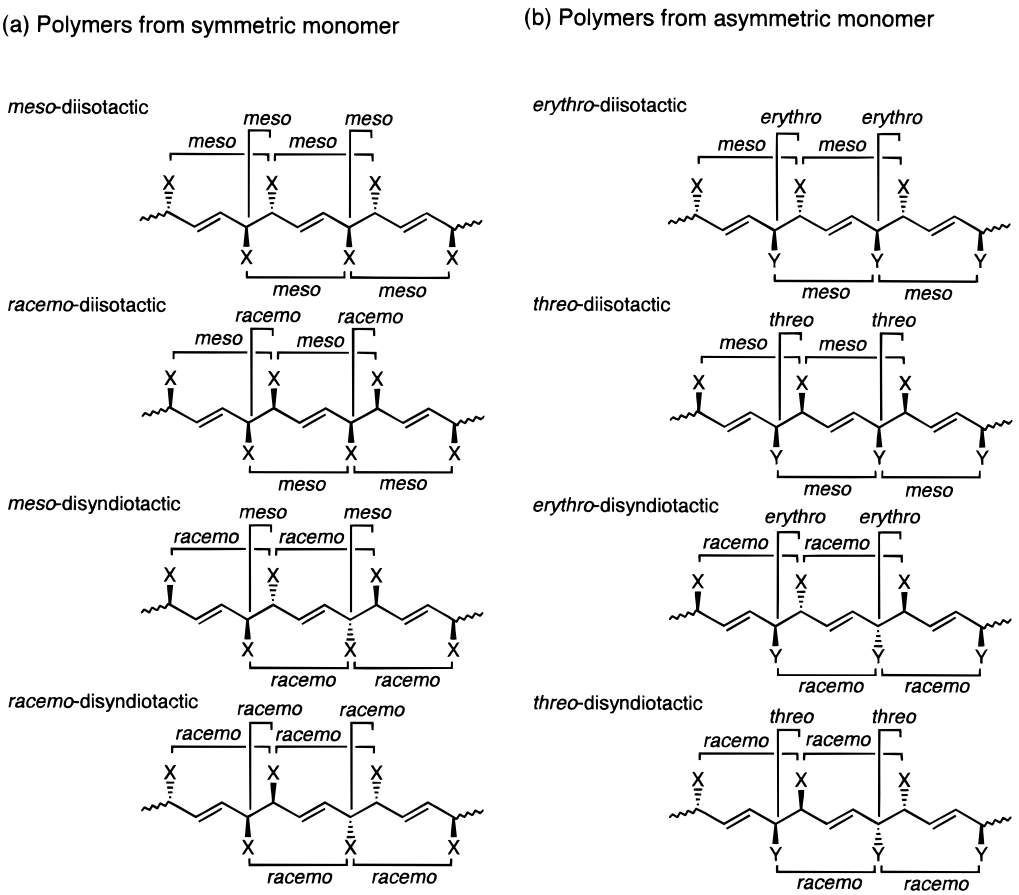

Figure 9. Stereoregular polymer sequences for *trans*-1,4-polymers obtained from (a) symmetric and (b) asymmetric 1,4-disubstituted butadienes. Dialkyl muconates and dialkylammonium muconates belong to the former. Alkylammonium monomethyl muconate and alkylammonium sorbate belong to the latter.

Table 5. Characteristic Distances and Angles for the Molecular Stacking in the Crystals of the Diene Monomers that Proceed Topochemical Polymerization[a]

crystal	d_{cc} (Å)	d_s (Å)	θ_1 (deg)	θ_2 (deg)
6	5.37	4.99	28	47
1c	4.19	4.94	80	52
diethyl *(Z,Z)*-muconate	3.79	4.93	85	49

[a] d_{cc} is the intermolecular carbon-to-carbon distance between double bonds that react during the topochemical polymerization. d_s is the stacking distance. θ_1 and θ_2 are tilt angles of the stacking. See Figure 8 for the definition of these parameters.

the topochemical polymerization and the stacking distance, respectively, as shown in Figure 8. The angles between the stacking direction and the molecular plane in orthogonally different directions are represented by θ_1 and θ_2. As indicated by the arrows in the side view of the 1,3-diene molecular planes of **6** in Figure 8a, the carbon-to-carbon distance is an appropriate value ($d_{cc} = 5.37$ Å) for the carbons that make new bonds to yield an *erythro*-diisotactic-2,5-*trans*-polymer during the topochemical polymerization. However, this distance value is slightly larger than those determined for the crystals of the polymerizable muconates. Furthermore, a smaller θ_1 value for **6** suggests the disadvantage of the interaction between the π-orbitals during the polymerization, whereas the θ_2 values were identical to each other ($\sim$50°). A larger d_{cc} or smaller θ_1 value seems to be unfavorable for the topochemical polymerization, but **6** actually polymerizes at a greater rate than **1c**. This is interpreted by the difference in the structures of the sorbate and muconates in the crystals. Both ends of the muconate dianions are linked to the hydrogen bond networks and sandwiched by the alkylammonium cation layers. In contrast, the monofunctional sorbate anions are fixed on the hydrogen bond network only at one side of the molecules. The methyl groups of the sorbate interact with each other as a weak van der Waals interaction in the crystals. The conformation in the diene moiety of **6** readily changes when it reacts to make new bonds. We are now continuing our efforts in the detailed and quantitative analysis of the molecular packing in the crystals and the establishment of a general rule to predict polymerization behavior and reactivity[26] based on the single-crystal structure of polymerizable and unpolymerizable monomers for a variety of diene derivatives.

Polymer Stereochemistry Determined by Crystal Structure. There are four types of possible stereoregular structures for each *trans*-1,4-polymer of 1,4-disubstituted butadiene.[27] Here, the substituted butadienes are classified into two groups, symmetrical monomers such as **1** and **2** (Figure 9a) and asymmetrical monomers such as **5** and **6** (Figure 9b). The stereochemistry of these polymers is represented by two kinds of relationships as follows, one of which is the relative configuration between the two repeating monomer units: when all the repeating relations are *meso*, the polymer is diisotactic, and when they are *racemo*, it is disyndiotactic.[28] Another relationship is the relative configuration between the vicinal carbon centers, being also represented by the same term, *meso* and *racemo* for a symmetrical structure, or by another term, *erythro* and *threo* for an asymmetric structure.

(26) For the general rule of the topochemical polymerization of diacetylenes, see ref 4c.

(27) Ordian, G. *Principles of Polymerization*, 3rd ed.; Wiley: New York, 1991; Chapter 8.

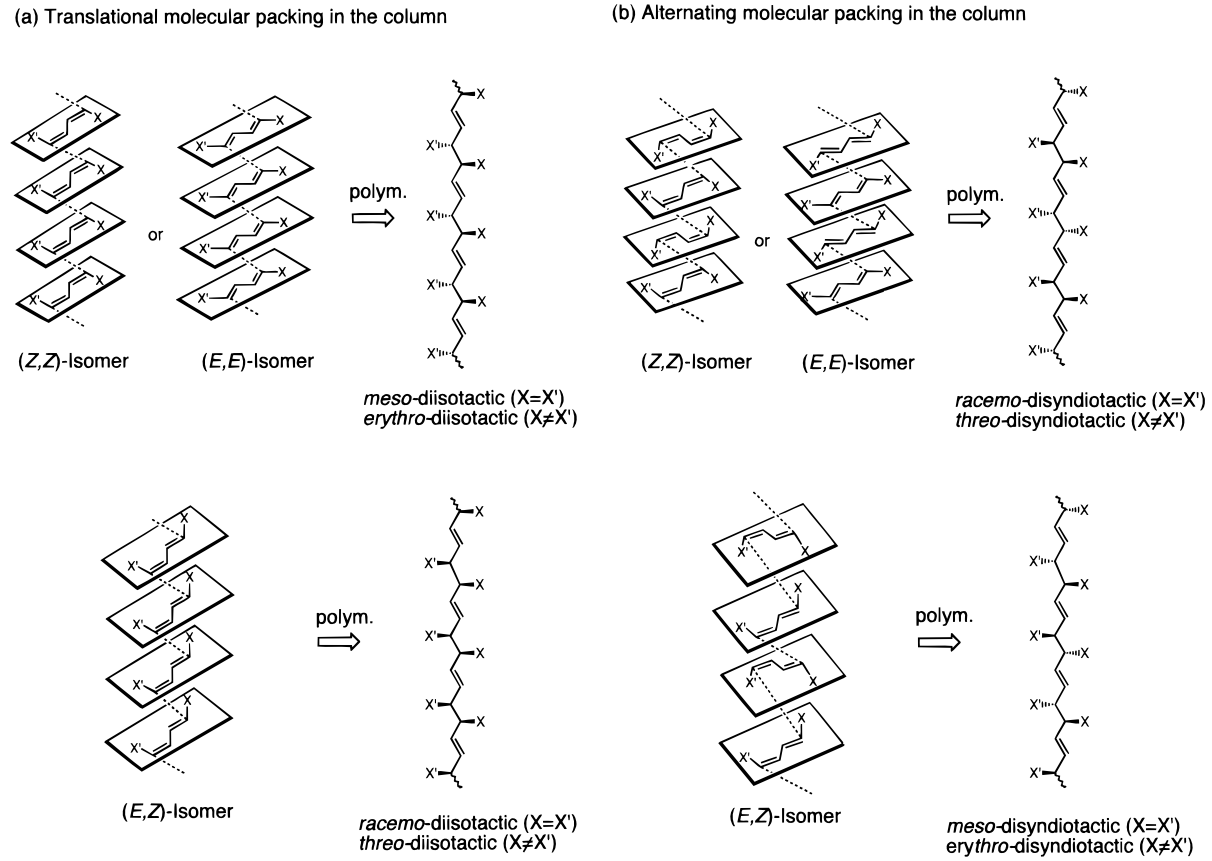

Figure 10. Relationship between the crystal packing of monomer molecules with different configurations and the stereochemical structure of polymers produced during topochemical polymerization of 1,4-disubstituted butadienes. (a) Translational molecular packing in the column. (b) Alternating molecular packing in the column.

Among the stereoregular polymers shown in Figure 9, the *racemo*-diisotactic polymer and the *erythro*- and *threo*-diisotactic polymers are chiral and possess optical activity, while the *meso*-diisotactic and *racemo*-disyndiotactic polymers are achiral because they possess a mirror plane in the chain. Three other polymers, the *meso*-disyndiotactic, *erythro*-disyndiotactic, and *threo*-disyndiotactic polymers have no mirror plane, but they are not optically active because of the existence of a mirror glide plane. All the polymers obtained in this study have been revealed to be of similar stereoregularity, i.e., a *meso*- or *erythro*-diisotactic structure. Therefore, we examined the optical activity of the polymers obtained from **5** or **6**. When the specific rotatory power of poly(**8**) and poly(**9**) in methanol was checked, we could not find any significant value for optical rotation. When a monomer crystal has a mirror plane or mirror glide plane, each optically active polymer of the right- and left-handed configurations is produced in the crystal, as shown in Scheme 7. A mixture of equimolar chiral crystals also provides a similar result. It is concluded that the presence of a mirror glide plane in the crystal of **6** is the reason the polymer has no optical activity, because the space group of the crystal of **6** is *C*2/*c*. The synthesis of the asymmetric carbon centers without any chiral auxiliary group or any external chiral agent has been one of the most intriguing topics in the fields of not only organic synthesis and crystallography but also life science because of

Scheme 7

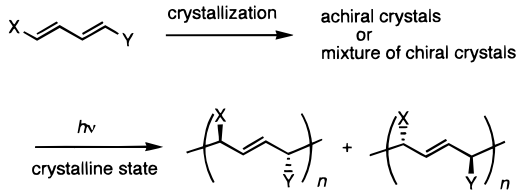

the importance of the origin of optical activity.[29] At the present time, we have not yet obtained any evidence for the formation of optically active polymers. Further crystallographic design for the monomer crystal structure would allow the possible synthesis of absolute asymmetry.

The stereochemical structure of the polymers produced during the topochemical polymerization is considered on the basis of the *EZ*-configuration and the stacking of the monomers. When monomer molecules translationally stack in a column in the crystals, both the *(Z,Z)*- and *(E,E)*-isomers provide an identical polymer, the *meso*- or *erythro*-diisotactic polymer, irrespective of the monomer configuration (Figure 10a). Here, the dotted lines tie the carbons which make a new bond during polymerization. The other type of stereoregular polymer such as the *racemo*- or *threo*-diisotactic polymer could be obtained if the topochemical polymerization of an *(E,Z)*-butadiene monomer

(28) In some polymer science textbooks, the terms *meso* and *racemic* are used. However, the IUPAC committee on nomenclature recommends the use of "*racemo*" but not "*racemic*". See, IUPAC Macromolecular Division, Commission on Macromolecular Nomenclature. *Compendium of Macromolecular Nomenclature*, Blackwell Scientific Publications: Oxford, 1991. See also: *Pure Appl. Chem.* **1981**, *53*, 733−752.

(29) (a) Addadi, L.; van Mil, J.; Lahav, M. *J. Am. Chem. Soc.* **1982**, *104*, 3422−3429. (b) Chung, C. M.; Hasegawa, M. *J. Am. Chem. Soc.* **1991**, *113*, 7311−7316. (c) Sakamoto, M. *Chem. Eur. J.* **1997**, *3*, 684−689. (d) Mason, S. F. *Nature* **1984**, *311*, 19−23. (e) Vaida, M.; Poporitz-Biro, R.; Leiserowitz, L.; Lahav, M. *Photochemistry in Organized and Constrained Media*; Ramamurthy, V., Ed.; VCH: New York, 1991; Chapter 6, pp 247−302.

proceeds with a similar mechanism. Actually, however, we have found no polymerization of any *(E,Z)*-monomer at the present time. Asymmetric molecules seem not to favor a simple columnar structure. Auxiliary groups other than a naphthylmethylammonium group are necessary for the topochemical polymerization of the *(E,Z)*-butadienes to give another type of stereoregular polymer. We have already shown that the photoirradiation of **3** in the crystalline state leads to the polymerization of **2** that was produced by the isomerization. If the molecules of **3** participate in the polymerization of **2**, i.e., the copolymerization of **2** with **3** occurs during the photoirradiation, the stereochemistry of the resulting polymer would be different from that of poly(**2**). Therefore, we checked the NMR spectrum of the polymer obtained from **3** via the isomerization−polymerization (run 8 in Table 1). It was of an atactic polymer as expected (Figure 2d). This indicates that the polymerization proceeded in the crystals of **2** containing **3** as the starting monomer. The solid solution of the *(Z,Z)*- and *(E,Z)*-derivatives formed during the isomerization makes it possible to obtain a polymer with a different type of stereochemical sequence (Scheme 5). On the other hand, the polymerization of **4** via the isomerization to **5** (run 10 in Table 1) resulted in the formation of a tritactic polymer because both **4** and **5** provide the identical stereochemical structure polymers (Scheme 6).

Differing from the diisotactic polymers, the disyndiotactic polymers are not obtained from the crystals with a translational molecular packing. An alternating molecular packing as shown in Figure 10b could result in the formation of disyndiotactic polymers, but such an alternating structure is unfavorable in actual crystals unless there is a particular interaction between the stacking monomers to support their structure. For this purpose, any alternating directivity of substituents, which never disturbs the columnar structure formation appropriate for topochemical polymerization, is indispensable. One of our subjects in the future is the design of monomer crystals to obtain various types of stereoregular polymers.

Conclusion. We have found that topochemical polymerization is efficiently induced by the introduction of a naphthylmethylammonium moiety as the countercation into the 1,3-diene mono- and dicarboxylate derivatives. The polymerization proceeded for not only the *(Z,Z)*-muconic acid derivatives, but also the *(E,E)*-muconic and sorbic acid derivatives, because the naphthylmethylammonium group is suitable for the formation of the columnar structure in the crystals. In the powder X-ray diffraction profile of the topochemically polymerizable crystals, a peak due to the lamella structure, consisting of the 1,3-diene carboxylate anion layers and the naphthylmethylammonium cation layers, was detected in the low-angle region. Such a lamella structure is one of the characteristic features of the monomer crystals that proceed through topochemical polymerization and was retained in the polymer crystals after polymerization. We also determined the single crystal structure of the sorbate and compared it with those of the previously reported muconates. It has been confirmed that the columnar-type structure formed by the appropriate stacking of the diene moieties induces the topochemical polymerization resulting in the stereoregular polymers. Further crystallographic study including the crystal structure analysis of the monomer and polymer crystals for various kinds of compounds will give us more detailed information about the intermolecular distance and angle parameters which determine the reactivity of the topochemical polymerization in the crystalline state.

On the basis of the consideration of the molecular packing model in the crystals, it has been revealed that the *(Z,Z)*- and *(E,E)*-isomers provide a *meso*- or *erythro*-diisotactic polymer, while an *(E,Z)*-isomer would give a *racemo*- or *threo*-diisotactic polymer. It also suggested the difficulty in crystal design for syndiotactic control, but this is one of our challenging subjects for the future. Topochemical polymerization in the crystalline state is undoubtedly one of the most powerful methods for the control of the polymer chain structure as well as the polymer crystal structure. The concept of crystal engineering has been renewed as a strategy for the rational design of organic architecture with the aid of the supramolecular synthon idea and it will reveal the more detailed characteristic features of the topochemical polymerization of the diene compounds. The polymer crystals obtained by topochemical polymerization have great potential as new organic solid materials for various applications. Polymer crystal engineering will be helpful for the design and control of the structure and functions of the organic solids.

Experimental Section

Materials. The monomers were prepared from the corresponding acid and alkylamine, followed by recrystallization from an appropriate solvent. *(Z,Z)*-Muconic acid was supplied from Mitsubishi Chemical Co. Ltd., Tokyo. The *(Z,Z)*-acid provided the *(E,Z)*- and *(E,E)*-muconic acids by heating and photoirradiation in solution, respectively.[30] Namely, an aqueous solution of the *(Z,Z)*-acid was refluxed for 6 h, then cooled to room temperature to precipitate the isomer *(E,Z)*-muconic acid. *(E,E)*-Muconic acid was obtained as the precipitant during the reaction when the *(Z,Z)*-acid was photoirradiated in methanol in the presence of iodine for 4 h, followed by recrystallization from methanol. The solubility of the acids in water or methanol was dependent on the *EZ*-configuration of the diene moiety, resulting in the easy separation of the isomers, e.g., the *(E,Z)*-acid was precipitated in water upon cooling after the thermal isomerization, and the *(E,E)*-acid was isolated as crystals during the photoirradiation in methanol due to the poor solubility. **1**−**3** were prepared from the corresponding isomer of muconic acid with an amine in quantitative yield. The structure of all monomers was checked by NMR, IR, and UV spectroscopies. The recrystallization of these compounds in an appropriate solvent gave powdery or thin-needle crystals.

Di(1-naphthylmethylammonium) *(Z,Z)*-muconate (1a): powder (methanol); mp 177 °C dec; ^{1}H NMR (400 MHz, CD_3OD) δ 8.10 (d, J = 8.5 Hz, Ar, 2H), 7.94 (t, J = 8.5 Hz, Ar, 4H), 7.4−7.7 (m, Ar, 8H), 7.4−7.5 (m, C*H*=CHCO$_2$, 2H), 5.90 (m, CH=C*H*CO$_2$, 2H), 4.54 (s, CH_2, 4H); IR (KBr) 1585 ($\nu_{C=C}$), 1504 ($\nu_{C=O}$) cm^{-1}; UV (CH_3OH) λ 261 nm (ϵ = 20 200).

Di((*S*)-1-naphthylethylammonium) *(Z,Z)*-muconate (1b): powder (ethanol); mp 140 °C dec; ^{1}H NMR (400 MHz, CD_3OD) δ 7.85−8.15 (m, Ar, 6H), 7.5−7.7 (m, Ar, 8H), 7.3−7.5 (br, C*H*=CHCO$_2$, 2H), 5.89 (m, CH=C*H*CO$_2$, 2H), 5.31 (q, J = 8.4 Hz, CH, 2H), 1.71 (d, J = 6.8 Hz, CH_3, 6H); ^{13}C NMR (100 MHz, D_2O) δ 176.48 (C=O), 134.68 (Ar), 134.45 (Ar), 131.31 (Ar), 131.31 (C=C), 130.47 (Ar), 130.19 (Ar), 130.01 (C=C), 128.13 (Ar), 127.39 (Ar), 126.49 (Ar), 123.53 (Ar), 122.85 (Ar), 47.15 (CH), 20.39 (CH_3); IR (KBr) 1585 ($\nu_{C=C}$), 1546 ($\nu_{C=O}$) cm^{-1}; UV (H_2O) λ 260 nm (ϵ = 21800).

Di(benzylammonium) *(Z,Z)*-muconate (1c): needles (methanol); mp 134 °C dec; ^{1}H NMR (400 MHz, D_2O) δ 7.32 (m, Ar, 10H), 6.80 (m, C*H*=CHCO$_2$, 2H), 5.82 (m, CH=C*H*CO$_2$, 2H), 4.05 (s, CH_2, 4H); ^{13}C NMR (100 MHz, D_2O) δ 176.45 (C=O), 133.46 (Ar), 131.31 (C=C), 130.27 (Ar), 130.06 (C=C), 130.06 (Ar), 129.66 (Ar), 43.94 (CH_2); IR (KBr) 1586 ($\nu_{C=C}$), 1506 ($\nu_{C=O}$) cm^{-1}; UV (H_2O) λ 257 nm (ϵ = 16 300).

Di(dodecylammonium) *(Z,Z)*-muconate (1d): powder (methanol); mp 109 °C dec; ^{1}H NMR (400 MHz, CD_3OD) δ 7.33 (m, C*H*=CHCO$_2$, 2H), 5.90 (m, CH=C*H*CO$_2$, 2H), 2.88 (t, J = 7.3 Hz, CH_2, 4H), 1.63 (m, CH_2, 4H), 1.2−1.5 (m, CH_2, 36H), 0.88 (t, J = 6.8 Hz, CH_3, 6H); ^{13}C NMR (100 MHz, CD_3OD) δ 175.20 (C=O), 132.85 (C=C), 130.84

(30) Elvidge, J. A.; Linstead, R. P.; Sims, P.; Orkin, B. A. *J. Chem. Soc.* **1950**, 2235−2241.

(C═C), 40.72 (CH_2), 33.09 (CH_2), 30.78 (CH_2), 30.69 (CH_2), 30.54 (CH_2), 30.51 (CH_2), 30.28 (CH_2), 28.75 (CH_2), 27.53 (CH_2), 23.76 (CH_2), 14.46 (CH_3); IR (KBr) 1590 ($\nu_{C=C}$), 1500 ($\nu_{C=O}$) cm^{-1}; UV (CH_3OH) λ 258 nm (ϵ = 15 700).

Di(octadecylammonium) *(Z,Z)*-muconate (1e): powder (ethanol); mp 122 °C dec; ^{1}H NMR (400 MHz, CD_3OD) δ 7.45 (m, C*H*═$CHCO_2$, 2H), 5.91 (m, CH═C*H*CO_2, 2H), 2.88 (t, J = 7.8 Hz, CH_2, 4H), 1.63 (m, CH_2, 4H), 1.1−1.5 (br, CH_2, 60H), 0.89 (t, J = 6.8 Hz, CH_3, 6H); IR (KBr) 1590 ($\nu_{C=C}$), 1500 ($\nu_{C=O}$) cm^{-1}; UV (CH_3OH) λ 258 nm (ϵ = 18 400).

Di(1-naphthylmethylammonium) *(E,E)*-muconate (2): powder (methanol); mp 221 °C dec; ^{1}H NMR (400 MHz, CD_3OD) δ 8.10 (d, J = 8.5 Hz, Ar, 2H), 7.94 (t, J = 8.5 Hz, Ar, 4H), 7.4−7.6 (m, Ar, 8H), 7.10 (m, C*H*═$CHCO_2$, 2H), 6.14 (m, CH═C*H*CO_2, 2H), 4.55 (s, CH_2, 4H); IR (KBr) 1615 ($\nu_{C=C}$), 1509 ($\nu_{C=O}$) cm^{-1}; UV (CH_3OH) λ 261 nm (ϵ = 25 100).

Di(1-naphthylmethylammonium) *(E,Z)*-muconate (3): powder (methanol); mp 140 °C dec; ^{1}H NMR (400 MHz, CD_3OD) δ 7.9−8.2 (m, Ar, 6H), 8.0−8.2 (m, CH═$CHCO_2$, 1H), 7.4−7.7 (m, Ar, 8H), 6.35 (t, J = 11.2 Hz, CH═$CHCO_2$, 1H), 5.90−6.05 (m, CH═$CHCO_2$, 2H), 4.57 (s, CH_2, 4H); IR (KBr) 1601 ($\nu_{C=C}$), 1556 ($\nu_{C=O}$) cm^{-1}; UV (CH_3OH) λ 261 nm (ϵ = 27 000).

The *(Z,Z)*-muconic acid monomethyl ester was prepared by the oxidation of catechol in the presence of methanol using CuCl as the catalyst according to the method reported in the literature.[31] The obtained acid monomethyl ester was found to contain a small amount of an *(E,Z)*-isomer and the content of the isomer increased upon heating the solution during the isolation process of the *(Z,Z)*-acid monomethyl ester after the reaction. The acid was converted into **4** by the quantitative reaction with the amine, similar to the synthesis of **1**. The isolated **4** also contained the *(E,Z)*-isomer as the impurity, but it was used in this study without further purification. On the other hand, **5** was obtained as the pure isomer by the isomerization of the *(Z,Z)*-acid monomethyl ester to the *(E,E)*-one and the subsequent salt formation. The *(E,E)*-muconic acid monomethyl ester was isolated by the photoirradiation of the corresponding *(Z,Z)*-acid in dichloromethane or methanol in the presence of iodine at room temperature for 8 h. After isomerization, the solvent and iodine were removed under reduced pressure. The residue was allowed to react with 1-naphthylmethylamine. **5** was isolated by recrystallization from methanol.

***(Z,Z)*-Muconic acid monomethyl ester:** needles (*n*-hexane); mp 78−79 °C; ^{1}H NMR (400 MHz, $CDCl_3$) δ 8.01 (t, J = 12.2 Hz, CH═C*H*CO_2, 1H), 7.87 (t, J = 11.6 Hz, CH═C*H*CO_2, 1H), 6.03 (dd, J = 11.2 and 4.4 Hz, C*H*═$CHCO_2$, 2H), 3.77 (s, CH_3, 3H); IR (KBr) 1718 ($\nu_{C=O}$), 1686 ($\nu_{C=O}$), 1587 ($\nu_{C=C}$) cm^{-1}.

***(E,E)*-Muconic acid monomethyl ester:** ^{1}H NMR (400 MHz, $CDCl_3$) δ 7.42 (m, CH═C*H*CO_2, 1H), 7.34 (m, CH═C*H*CO_2, 1H), 6.24 (t, J = 15.4 Hz, C*H*═$CHCO_2$, 2H), 3.80 (s, CH_3, 3H).

Methyl 1-naphthylmethylammonium *(Z,Z)*-muconate (4): powder (methanol); mp 124−126 °C; ^{1}H NMR (400 MHz, CD_3OD) δ 8.10 (d, J = 8.8 Hz, Ar, 1H), 7.96 (d, J = 10.4 Hz, Ar, 2H), 7.5−7.7 (m, CH═C*H*CO_2 and Ar, 6H), 6.12 (d, J = 10.4 Hz, C*H*═$CHCO_2$, 1H), 5.78 (d, J = 12.0 Hz, C*H*═$CHCO_2$, 1H), 4.60 (s, CH_2, 2H), 3.70 (s, CH_3, 3H); IR (KBr) 1713 ($\nu_{C=O}$), 1631 ($\nu_{C=O}$), 1585 ($\nu_{C=C}$) cm^{-1}.

Methyl 1-naphthylmethylammonium *(E,E)*-muconate (5): powder (methanol); ^{1}H NMR (400 MHz, CD_3OD) δ 8.10 (d, J = 8.4 Hz, Ar, 1H), 7.96 (d, J = 8.0 Hz, Ar, 2H), 7.5−7.7 (m, Ar, 4H), 7.31 (dd, J = 15 and 12 Hz, CH═C*H*CO_2, 1H), 7.06 (dd, J = 15 and 12 Hz, C*H*═$CHCO_2$, 1H), 6.26 (d, J = 15.6 Hz, C*H*═$CHCO_2$, 1H), 6.13 (d, J = 15.6 Hz, C*H*═$CHCO_2$, 1H), 4.61 (s, CH_2, 2H), 3.74 (s, CH_3, 3H); IR (KBr) 1710 ($\nu_{C=O}$), 1638 ($\nu_{C=O}$), 1612 ($\nu_{C=C}$) cm^{-1}; UV (CH_3OH) λ 262 nm (ϵ = 38 900).

Monomers **6** were prepared from a commercial *(E,E)*-sorbic acid and the amine, followed by recrystallization from methanol to provide needle crystals.

1-Naphthylmethylammonium *(E,E)*-sorbate (6): needles (methanol); mp 108 °C dec; ^{1}H NMR (400 MHz, CD_3OD) δ 7.34 (m, Ar, 5H), 7.01 (dd, J = 15.6 and 11.8 Hz, C*H*═$CHCO_2$, 1H), 6.17 (m, C*H*═$CHCH_3$, 1H), 6.02 (m, CH═C*H*CH_3, 1H), 5.78 (d, J = 15.6 Hz, CH═C*H*CO_2, 1H), 4.05 (s, CH_2, 2H), 1.67 (d, J = 6.0 Hz, CH_3, 3H); ^{13}C NMR (100 MHz, CD_3OD) δ 175.71 (C═O), 142.07 (C═C), 136.45 (C═C), 135.39 (Ar), 132.36 (Ar), 131.72 (Ar), 131.27 (Ar), 130.76 (C═C), 130.04 (Ar), 128.39 (Ar), 128.18 (Ar), 127.41 (Ar), 126.78 (Ar), 126.52 (Ar), 123.75 (C═C), 41.46 (CH_2), 18.54 (CH_3); IR (KBr) 1626 ($\nu_{C=C}$), 1507 ($\nu_{C=O}$) cm^{-1}; UV (CH_3OH) λ 251 nm (ϵ = 13 100).

Photoreaction. The monomer crystals were photoirradiated with a high-pressure mercury lamp at a distance of 10 cm under atmospheric conditions at room temperature. After irradiation, the polymer was isolated by removing the unreacted monomer with methanol. The polymer yield was gravimetrically determined. The isomer composition of the recovered monomers was determined by ^{1}H NMR spectroscopy.

Polymer Transformation. The hydrolysis of the polymers was carried out by soaking in HCl methanol (ca. 1 M) at room tempearture for 30 min and the mixture was filtered and washed with methanol to yield the corresponding acid polymer.

Poly(muconic acid): IR (KBr) 1714 ($\nu_{C=O}$) cm^{-1}. Anal. Calcd for $(C_6H_6O_4)_n$: C, 50.71; H, 4.26. Found: C, 50.42; H, 4.29.

Poly(muconic acid monomethyl ester): IR (KBr) 1740 ($\nu_{C=O}$), 1705 ($\nu_{C=O}$) cm^{-1}.

Poly(sorbic acid): IR (KBr) 1716 (νC═O) cm^{-1}. Anal. Calcd for $(C_6H_8O_2)_n$: C, 64.26; H, 7.21. Found: C, 64.05; H, 7.36.

To the polymeric acid was added an excess triethylamine and methanol-d_4 in an NMR tube, and then the solution was provided for the NMR measurement. Similarly, the methanol solution of poly(**7**)−poly(**9**) was provided for the viscosity measurement.

Poly(7) derived from poly(1a): ^{13}C NMR (100 MHz, CD_3OD) δ 178.5 (C═O), 131.2 (C═C), 55.9 (CH), 47.0 (CH_2), 10.4 (CH_3).

Poly(7) derived from poly(2): ^{13}C NMR (100 MHz, CD_3OD) δ 178.6 (C═O), 131.2 (C═C), 56.0 (CH), 47.0 (CH_2), 10.7 (CH_3).

Poly(7) derived from atactic polymer obatined by isomerization polymerization of 3: ^{13}C NMR (100 MHz, CD_3OD) δ 179.0 (br, C═O), 131.4 (br, C═C), 56.7 (br, CH), 47.1 (CH_2), 11.1 (CH_3).

Poly(8) derived from poly(5): ^{13}C NMR (100 MHz, CD_3OD) δ 178.0 (C═O), 174.3 (C═O), 133.4 (C═C), 129.6 (C═C), 57.4 (CH), 54.8 (CH), 52.1 (OCH_3), 47.0 (CH_2), 10.5 (CH_3).

Poly(9) derived from poly(6): ^{13}C NMR (100 MHz, CD_3OD) δ 181.8 (C═O), 137.2 (C═C), 130.1 (C═C), 62.0 (CH), 39.7 (CH), 18.5 (CH_3), 46.9 (CH_2), 11.0 (CH_3).

Measurements. The IR and NMR spectra were recorded on JASCO FTIR-430 and JEOL JMN A-400 spectrometers, respectively. Intrinsic viscosity was determined in methanol or aqueous NaCl at 30 °C using an Ubbelohde-type viscometer. An optical rotation was determined with the D line from a sodium lamp in methanol at room temperature using a JASCO DIP-181 photometer. The powder X-ray diffraction data were collected using a Shimadzu XD-610 diffractometer with monochromatized Cu Kα radiation (λ = 1.5418 Å). Single-crystal X-ray data were collected on a Rigaku R-AXIS RAPID diffractometer using Mo Kα radiation monochromated by graphite. The structure was solved by the direct method with the program SAPI91 and refined by full-matrix least-squares procedures. All calculations were performed using the TEXSAN crystallographic software package of the Molecular Structure Corporation.

Acknowledgment. The authors acknowledge Dr. K. Sada and Profs. M. Miyata and K. Tashiro, Osaka University, for invaluable discussions and useful suggestions. The recent work was supported in part by a Grant-in-Aid for Scientific Research (No. 11650911) from the Ministry of Education, Science, Sports and Culture of Japan.

Supporting Information Available: ^{1}H NMR spectra of the monomers **1**−**6** and other compounds, ^{13}C NMR spectra of poly(**7**)-poly(**9**), powder X-ray diffraction profiles of the monomer and polymer crystals, and crystallographic data of **6** (PDF). This material is available free of charge via the Internet at http://pubs.acs.org.

JA001093N

(31) (a) Tsuji, J.; Takayanagi, H. *Tetrahedron* **1978**, *34*, 641−644. (b) Bankston, D. *Organic Syntheses*; Freeman, J. P., Ed.; Wiley: New York, 1993; Vol. VIII, pp 490−492.